



Carbon encapsulated mixed-metal sulfide as proficient electrocatalyst for hydrogen evolution reaction

Shahid Hussain¹ · Nabi Ullah³ · Yingyi Zhang² · Nimra Aslam⁴ · Asma Shaheen⁵ · Muhammad Sufyan Javed⁶ · Mingsong Wang¹ · Guiwu Liu¹ · Guanjun Qiao¹

Received: 6 February 2019 / Accepted: 8 July 2019 / Published online: 12 July 2019
© Springer Science+Business Media, LLC, part of Springer Nature 2019

Abstract

Proficient electrocatalyst for hydrogen evolution reaction (HER) synthesized via a single-step, simple and low-temperature pyrolysis method. The mixed metal sulfide catalyst $\text{Co}_9\text{S}_8/\text{NiS}@C$ shows irregular multi-shaped structure having small pores covered with carbon layers. The as-prepared $\text{Co}_9\text{S}_8/\text{NiS}@C$ composites are made up of very small intermingled nanoparticles. The tiny nanoparticle contains large surface area that serves as an active-site for excellent HER performances. The $\text{Co}_9\text{S}_8/\text{NiS}@C$ electrode is tested under alkaline solution performs overpotential (vs. RHE) of 0.28 V at current density of 10 mA cm^{-2} . It exhibits a low R_{ct} with an excellent and continuous stability for 10 h. The excellent HER performances of $\text{Co}_9\text{S}_8/\text{NiS}@C$ are attributed to shape, size, and crystal structure of mixed metal sulfide and small surface pores that provide abundant active sites for electrocatalysis reaction.

1 Introduction

Energy crises and climatic issues caused by the utilization of a limited source of fossil fuels divert the research direction toward sustainable and renewable energy source [1–5].

Hydrogen, being one of the most energy carriers has utmost potential to reduce climatic issues and energy crises due to its high energy density, renewability, sustainability, and carbon free-emissions [$2\text{H}_2 + \text{O}_2 \rightarrow 2\text{H}_2\text{O}$] [6–9]. Water electro-catalysis is an ideal and environmental friendly pathway to harvest pure hydrogen via hydrogen evolution reaction (RHE) [$2\text{H}_2\text{O} \rightarrow 2\text{H}_2 + \text{O}_2$] [6, 10–13]. For hydrogen evolution reaction, catalyst plays a vital role for outstanding performances. Platinum and platinum-based material are excellent electrocatalysts for HER due to their excellent kinetics and negligible overpotential, but their commercialization is thwarted by their intolerable price and scarcity in nature [14–17]. Thus, it is greatly imminent to design inexpensive, earth-plentiful and electroactive catalyst for HER systems [10, 18].

The transition metal such as Ni and Co and their derivatives have been widely investigated for ORR, HER and MOR applications due to their abundant availability and good catalytic nature [7, 11, 14, 19]. In the last few years, Ni and Co based sulfides have attained huge attention for HER properties because of low toxicity, excellent cyclic stability and superior electrocatalytic performances with excellent conductivity [11, 20–22]. There are only a few studies presented at recent for mixed metal sulfides behavior and its industrial usages. Ma et al. synthesized NiS–CoS nanorods by hydrothermal method, the obtained NiS–CoS nanorods exhibited a small overpotential of 102 mV at current density

Shahid Hussain and Nabi Ullah contributed equally to this work.

✉ Shahid Hussain
shahidsargodha@gmail.com

✉ Yingyi Zhang
zhangyingyi@cqu.edu.cn

✉ Mingsong Wang
wangms@mail.ujs.edu.cn

¹ School of Material Science and Engineering, Jiangsu University, Zhenjiang 212013, People's Republic of China

² School of Metallurgical Engineering, Anhui University of Technology, Maanshan 243002, Anhui, People's Republic of China

³ School of Chemistry and Chemical Engineering, Jiangsu University, Zhenjiang 212013, People's Republic of China

⁴ Department of Physics, University of Sargodha, Sargodha 40100, Pakistan

⁵ Department of Earth Sciences, University of Sargodha, Sargodha 40100, Pakistan

⁶ Department of Physics, COMSATS University Islamabad, Lahore Campus, Lahore 54000, Pakistan

of 10 mA cm^{-2} with Tafel value of 71 mV dec^{-1} for HER in 1 M KOH [23]. Zequine et al. prepared NiCo_2S_4 using hydrothermal method showing an overpotential of 148 mV at current density of 10 mA cm^{-2} with Tafel value of 119 mV dec^{-1} for HER in 1 M KOH [24]. Similarly, Subhasis et al. developed $\text{CoS}_x/\text{Ni}_3\text{S}_2/\text{NF}$ by hydrothermal method. The obtained electrocatalyst exhibited an overpotential value of 204 mV at a current density of 10 mA cm^{-2} with Tafel value of $133.3 \text{ mV dec}^{-1}$ for HER in 1 M KOH [25]. The aforementioned methods follow multi-step preparations and are difficult to control during the reaction system. Therefore, this area of research still requires plentiful research work to develop new efficient electrocatalysts for HER. In addition, there are only a few studies on mixed metal sulfide electrocatalyst for HER.

In this study, mixed metals of nickel and cobalt sulfide are prepared by simple and low-temperature pyrolysis method. The mixed metal sulfide exhibited outstanding HER electrocatalytic performance, obtaining a current density of 10 mA cm^{-2} at an overpotential of 0.28 V (vs. RHE) with small Tafel slope of 98 mV dec^{-1} . Both the nickel and cobalt sulfides are observed with multiple oxidation states with complex crystal structures. The overall excellent HER performances are accredited to metals oxidation phases, crystal structure and large surface area nanoparticles that provided plenty of electro- active sites in the reaction system. The present study may open new ways to synthesize different carbon encapsulated mix metal sulfide for HER electrocatalysts.

2 Experimental

2.1 Synthesis of $\text{Co}_9\text{S}_8/\text{NiS}@C$

Nickel acetate tetrahydrate [$\text{Ni}[(\text{CH}_3\text{COO})_2]\cdot 4\text{H}_2\text{O} \geq 98\%$], cobalt acetate tetrahydrate [$\text{Co}[(\text{CH}_3\text{COO})_2]\cdot 4\text{H}_2\text{O} \geq 99.5\%$] and thiourea [$\text{CS}(\text{NH}_2)_2 \geq 99\%$] purchased from Keshi Chemical Reagent Co., Ltd, China are used without additional refinement. One gram Nickel acetate, 1 g cobalt acetate, and 1 g thiourea were mixed in 20 mL DI water and magnetic stirred until a homogeneous solution is obtained. The homogeneous solution was then dried at $60 \text{ }^\circ\text{C}$ for 12 h and heated in a tube furnace at $600 \text{ }^\circ\text{C}$ for 60 min at a heating rate of $10 \text{ }^\circ\text{C min}^{-1}$ under N_2 gas flow. Next, the sample is air dried under room temperature conditions to obtain powders of $\text{Co}_9\text{S}_8/\text{NiS}@C$ composites. Similar procedure is followed to synthesize $\text{Ni/Co}@C$ electrocatalyst but without thiourea, for comparison.

2.2 Characterizations

The phase purity and crystal structure are analyzed using Bruker AXS Co.Ltd., Germany Advanced X-ray diffraction

(XRD). The structural morphologies are characterized by Hitachi S-4800 scanning electron microscopy (SEM) Japan and JEOL-JEM-2010 Japan transmission electron microscopy (TEM). The chemical compositions are confirmed by Thermo ESCALAB 250 X-ray photoelectron spectrometer (XPS). The specific surface area, pore volume, and pore size in the samples are characterized by Brunauer–Emmett–Teller (BET) NOVA2000e Quantachrome Corporation analytical system.

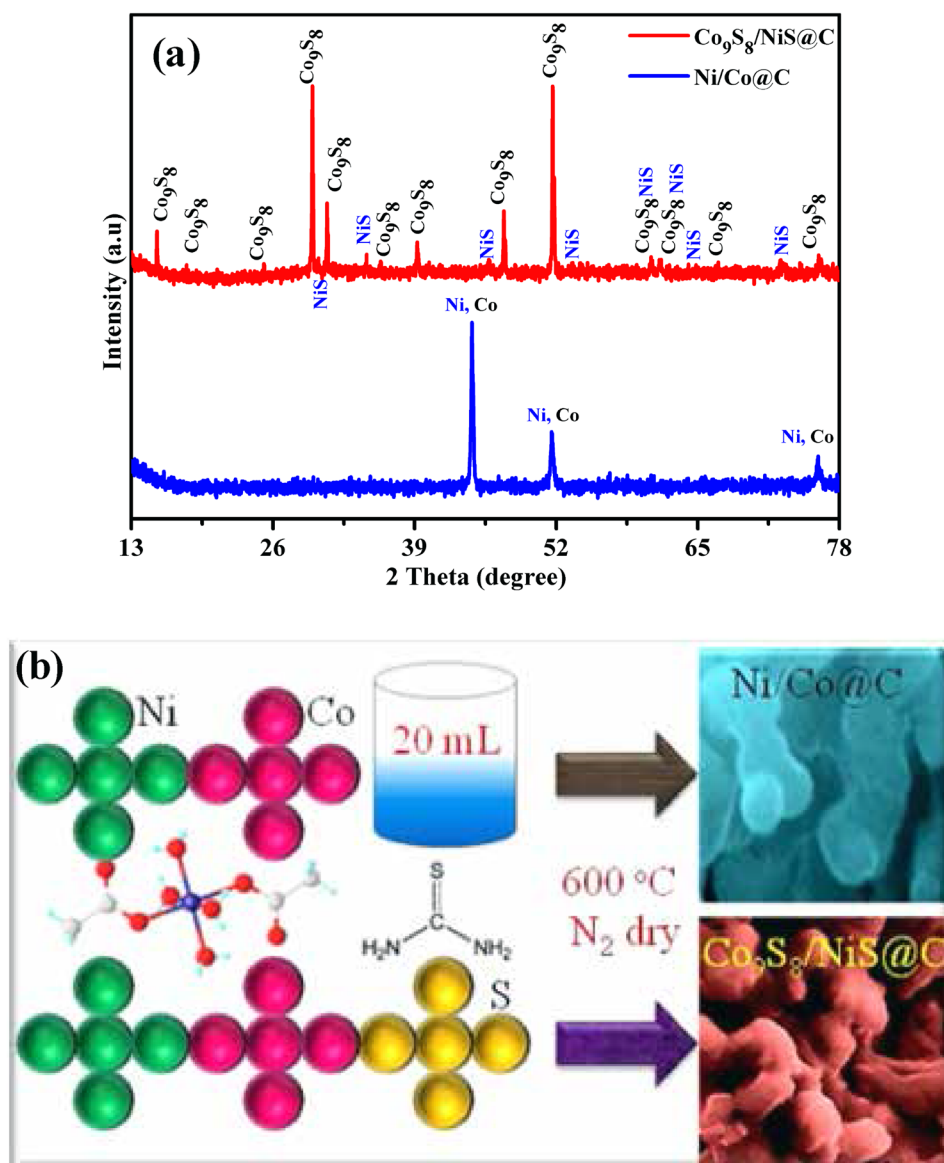
2.3 Electrochemical characterization

A CHI 760 electrochemical workstation containing three-electrode system is used to analyze electrochemical performances of the fabricated electrocatalysts. Mainly, saturated calomel electrode (SCE), glassy carbon electrode (GCE) and graphite rod were used as reference working, and counter electrodes, respectively. The electrode fabrication is as follows: 5 mg of the electrocatalyst is mixed in 750 μL (deionized water), 250 μL (ethanol) and 30 μL (5% Nafion), then mixture was sonicated for 30 min to gain uniform slurry. Following, 5 μL of ink was sprinkled on surface of working electrode and dried naturally. 1 M KOH electrolyte solution is purged for half hour with N_2 gas before electrochemical measurements. The Nernst equation ($E_{\text{RHE}} = E_{\text{SCE}} + 0.242 + 0.059 \times \text{pH}$) is employed to convert potential versus RHE. The electrocatalysts were stabilized and activated by cyclic voltammetry (CV) cycles at 100 mV s^{-1} scan rate. Linear sweep voltammetry (LSV) for HER was obtained at 5 mV s^{-1} in potential window of 0.0 to -0.4 V (vs. RHE). Electrochemical active surface areas (ECSA) of as-prepared catalysts are calculated from simple CV method. The CV curves are recorded at scan rates of 20, 40, 60, 80, and 100 mV s^{-1} at a range of 0.2 to 0.3 V (vs. RHE). The current density differences ($j_a - j_c$ (0.25 V)) are plotted versus the scan rates and the obtained slope which demonstrate ECSA which is generally taken as twice of the slope of electrochemical double-layer capacitances (Cdl). Electrochemical impedance spectroscopy (EIS) of the as-prepared catalysts were obtained at 5 mV AC amplitude in frequency range of 1 to 10^5 Hz at open circuit potential. The stabilities of electrocatalyst were analyzed by chronoamperometric at a potential of -0.2 V (vs. RHE) for 10 h.

3 Result and discussion

The XRD patterns shown in Fig. 1a confirm the phase purity of the pre-and final $\text{Co}_9\text{S}_8/\text{NiS}@C$ samples. XRD pattern of $\text{Co}_9\text{S}_8/\text{NiS}@C$ exhibited sharp peaks at 15.44° , 17.85° , 25.35° , 29.82° , 31.18° , 36.16° , 39.53° , 47.55° , 52.07° , 61.16° , 61.96° , 67.30° , and 76.74° corresponding to (111), (200), (220), (311), (222), (400), (331), (511), (440), (533),

Fig. 1 a XRD patterns and **b** formation mechanism of $\text{Co}_9\text{S}_8/\text{NiS}@C$ and $\text{Ni/Co}@C$ electro-catalysts



(622), (711), and (800) planes of face center cubic (FCC) Co_9S_8 [JCPDS # 65-6801] respectively. Similarly the peaks at 30.00° , 34.55° , 45.86° , 53.27° , 61.03° , 62.35° , 64.63° , and 72.88° are index to (100), (101), (102), (110), (103), (200), (112), and (202) planes of hexagonal NiS [JCPDS # 75-s0613] respectively. While, XRD pattern of $\text{Ni/Co}@C$ exhibited sharp peaks at 44.50° , 51.84° , and 76.37° and 44.21° , 51.52° , and 75.85° corresponding to (111), (200), and (220) plane of cubic face-centered Ni [JCPDS No. 04-0850] and cubic face-centered Co [JCPDS No. 15-0806], due to high similarity of Ni and Co, Ni overlapped Co peaks respectively. Carbon is in amorphous phase showing no obvious impurities peak in the sample.

The SEM images of $\text{Ni/Co}@C$ exhibited irregular multi-shaped macro-particles where the particles are wedged together forming a condense structure, as shown in Fig. 2.

The Ni and Co particles are covered by ultrathin carbon layers (Fig. 2a) which connect the metal particles. Similarly, $\text{Co}_9\text{S}_8/\text{NiS}@C$ exhibited the irregular shaped macro/nano-particles of Co_9S_8 and NiS which is covered by carbon layers (Fig. 2b), and may reduce the corrosion of metal and metal sulfide during the whole reaction system. The irregular and multi-shaped particles not only construct the porosity, but also increase the surface area of the sample and provide more active site for catalytic reaction. The pores provide easy paths and reservoir to ions and electrolyte for a close contact with metal and metal sulfide during instantaneous reaction enhancing HER. The TEM images of $\text{Co}_9\text{S}_8/\text{NiS}@C$ shows irregular particles like nanostructure of Co_9S_8 and NiS particles while gray sheet-like layers demonstrate the carbon served as an encapsulation for $\text{Co}_9\text{S}_8/\text{NiS}$. The light gray color of carbon is due to ultrathin structure of

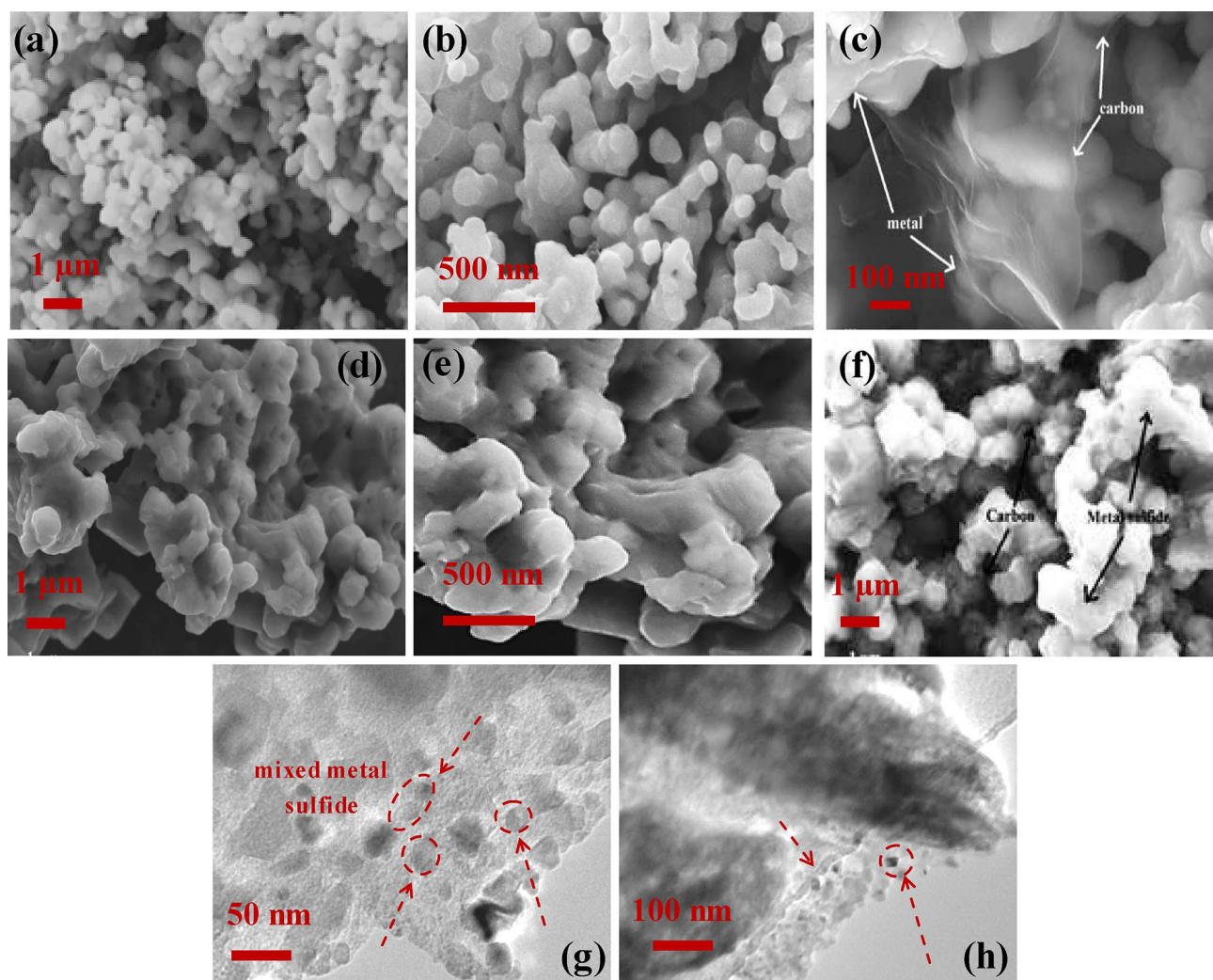


Fig. 2 a–f Low and high magnification SEM images of Ni/Co@C and Co₉S₈/NiS@C, and **g, h** TEM images of Co₉S₈/NiS@C

carbon layers. The irregular particles of Co₉S₈ and NiS are well spread in carbon which may reduce the agglomeration of metal nanoparticles as shown in Fig. 2c.

The uniform dispersion of metal and metal sulfide particles in ultrathin carbon layers provides wide electrochemical active surface area for hydrogen evolution reaction. Besides, the irregular nano-sized (7.2 to 23.5 nm) trapped mixed metal sulfide particles of Co₉S₈ and NiS are considered to be ideal for HER electrocatalytic reaction. The specific surface area, pore volume and pore size of the as-prepared samples are studied by nitrogen adsorption–desorption isotherm method. The Co₉S₈/NiS@C and Ni/Co@C show (Fig. 3a) the Brunauer–Emmett–Teller (BET) specific surface area of 58 and 60 m² g⁻¹, respectively. The BJH desorption (Fig. 3b, c) shows that Co₉S₈/NiS@C and Ni/Co@C exhibited pore volume of 0.342382 and 0.438344 cm³ g⁻¹ and pore size of 12.3406, 14.2582 nm, respectively. Both the samples exhibited almost same specific surface area, pore volume,

and pore size but with a minor difference Co₉S₈/NiS@C values than Ni/Co that might be due S content, which reduce the pore size, volume, and surface area of the sample. The total pore size distribution graph reflects mesoporous with large number of nano pores on the surface of, as shown in Fig. 3. The mesoporous structures and nano pores on the surface provide easy path for electrolyte and ion and slam intermingle to active site for catalytic reactions for improved for HER.

The chemical composition and state of elements of the as-prepared nanomaterials are recorded using XPS techniques. The survey spectrum (Fig. 4a) of Co₉S₈/NiS@C electrocatalyst confirmed the existence of Ni, Co, S, C, and O as shown in Fig. 4 respectively. The Gaussian fitting method was used to demonstrate Co 2p, Ni 2p, S 2p, O 1s and C 1s emission spectra of Co₉S₈/NiS@C composites. Figure 4b shows deconvoluted spectrum of Co 2p, the peaks fitted to two doublets spin–orbit with shake-up satellite, the 2p 3/2

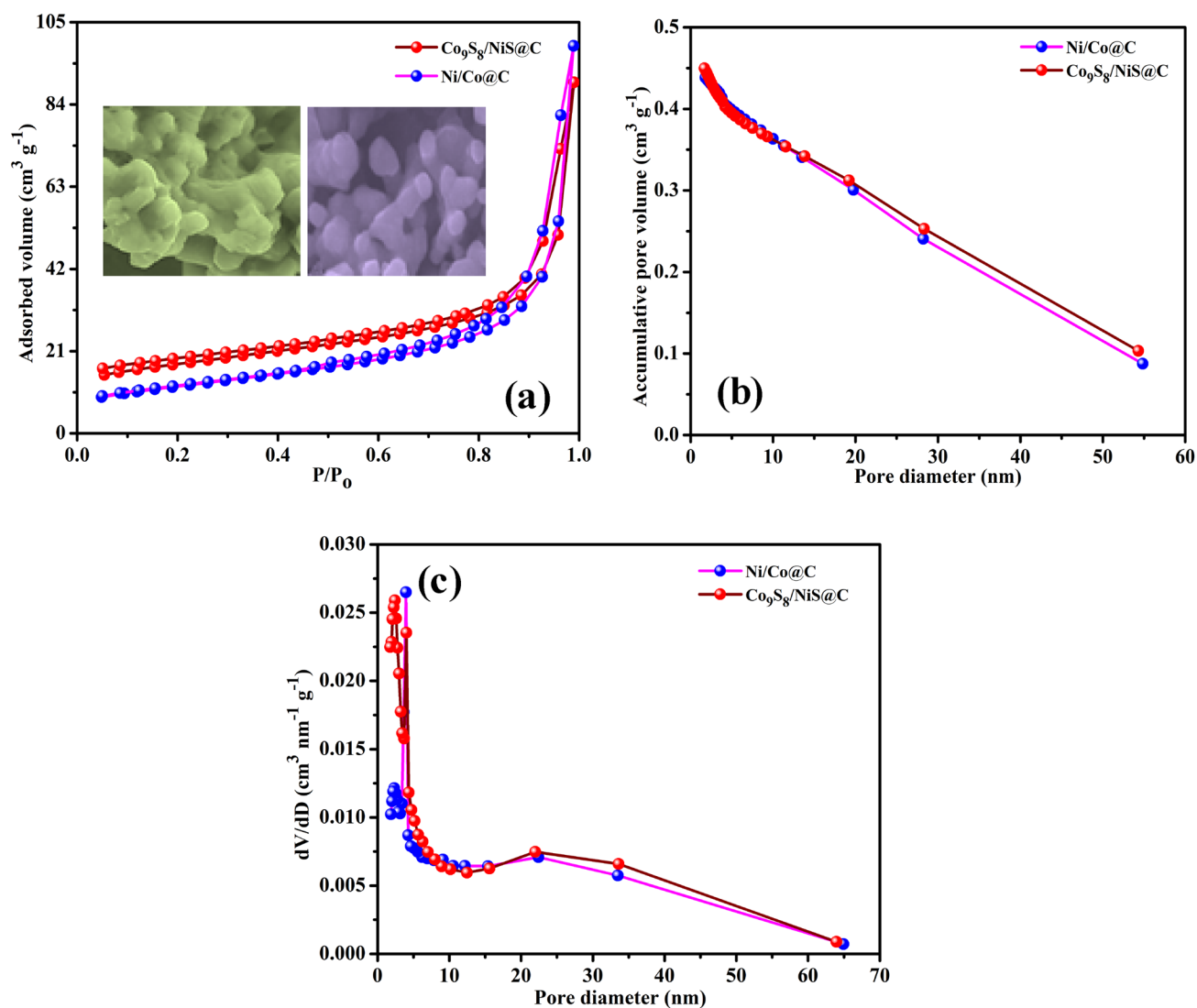


Fig. 3 **a** BET specific surface area, **b** pore volume and **c** pore size distribution of $\text{Co}_9\text{S}_8/\text{NiS}@C$

peaks at 778.17 and 781.33 eV with shake-up satellite at 784.80 eV, and 2p 1/2 peaks at 793.37 and 796.99 eV with shake-up satellite at 802.07 eV, are demonstrating Co^{3+} and Co^{2+} state of cobalt respectively. Similarly, the deconvoluted spectrum of Ni 2p (Fig. 4c) is fitted to doublet spin-orbit with shake-up satellites accordingly. The 2p 3/2 peak at 852.78 and 855.92 eV with shake-up satellite at 861.13 eV and 2p 1/2 peaks at 870.22 and 873.67 eV with shake-up satellite at 879.33 eV are corresponding to Ni^{2+} and Ni^{3+} state of Ni, respectively. In the deconvoluted spectra of S 2p, the 2p 3/2 and 2p 1/2 peaks at 161.12 and 162.1 eV with shake-up satellite at 168.37 eV are corresponding to metal and sulfide ion coordination, and the peak at 163.27 eV, is corresponding to carbon and sulfur bond, as shown in Fig. 4d [26, 27]. The O 1s spectra shown in Fig. 4e, fitted to three peaks around at 531.28, 532.11 and 535.42 eV corresponds

to surface metal oxide, and physically/chemically absorb oxygen, respectively. These oxides might be due to the contact of the sample surface with air to produce oxides on the surface, but the concentration of oxide on the surface is negligible and unable to detect in XRD. The fitted peak C 1s spectrum (Fig. 4f) at 284.60 eV corresponding to alternative C=C and C-C, while 286.20, 287.62 and at 289.08 eV corresponding to C-S, C-O and C=O bond, respectively [27].

The electrocatalytic HER performances of $\text{Co}_9\text{S}_8/\text{NiS}@C$ electrocatalyst were investigated using LSV in potential range 0 to 0.4 V (vs. RHE) under alkaline electrolytic (1 M KOH) solution at sweep rate of 5 mV. For comparison, Pt/C and $\text{Ni}/\text{Co}@C$ were also tested along with $\text{Co}_9\text{S}_8/\text{NiS}@C$, under the same conditions. Figure 5a shows LSV polarization curves with iR compensation for $\text{Co}_9\text{S}_8/\text{NiS}@C$, $\text{Ni}/\text{Co}@C$, and Pt/C catalysts, respectively. The LSV shows that

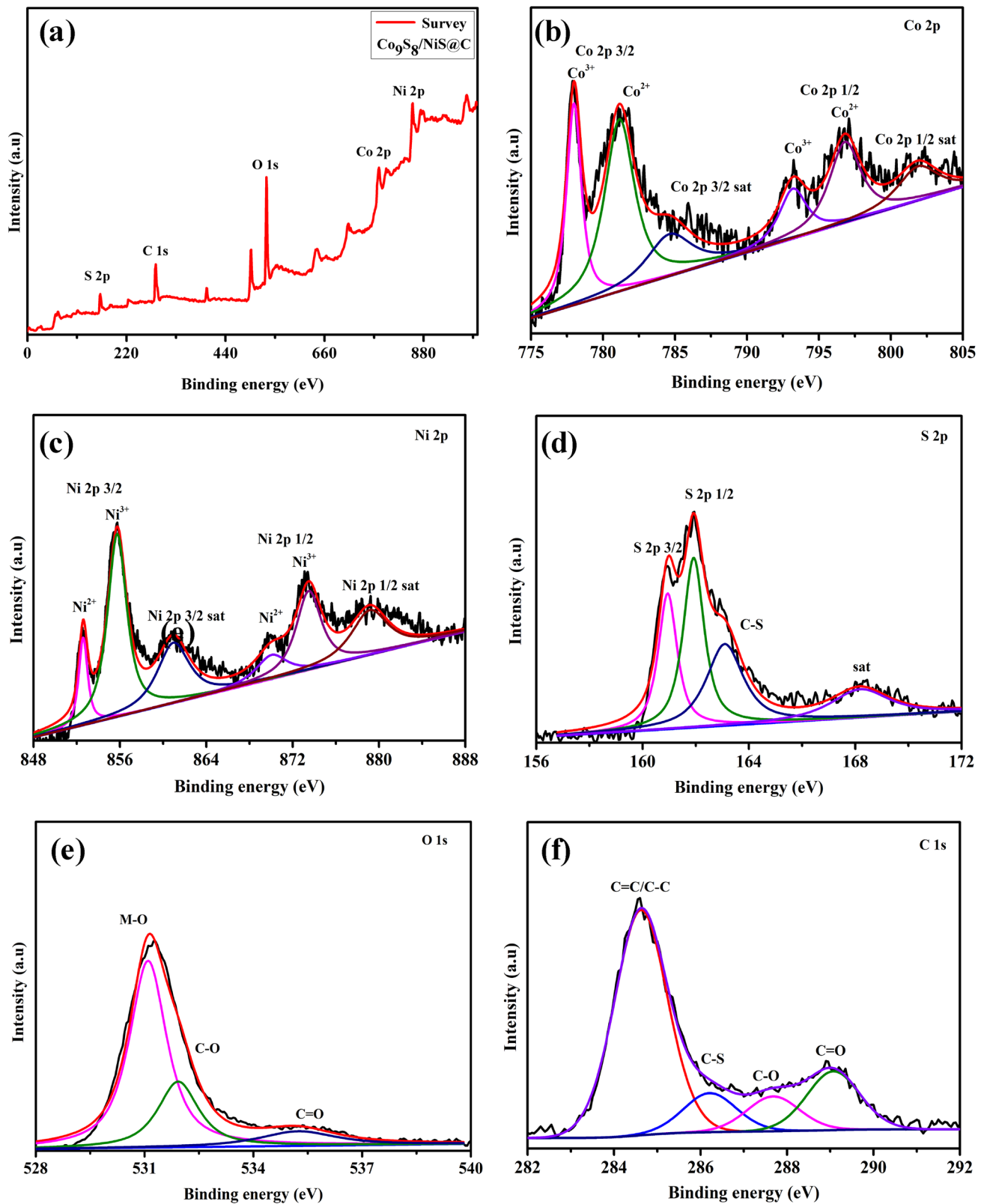


Fig. 4 XPS data of $\text{Co}_9\text{S}_8/\text{NiS}@C$: **a** survey spectra of elements, **b** Co 2p, **c** Ni 2p, **d** S 2p, **e** O 1s, **f** C 1s

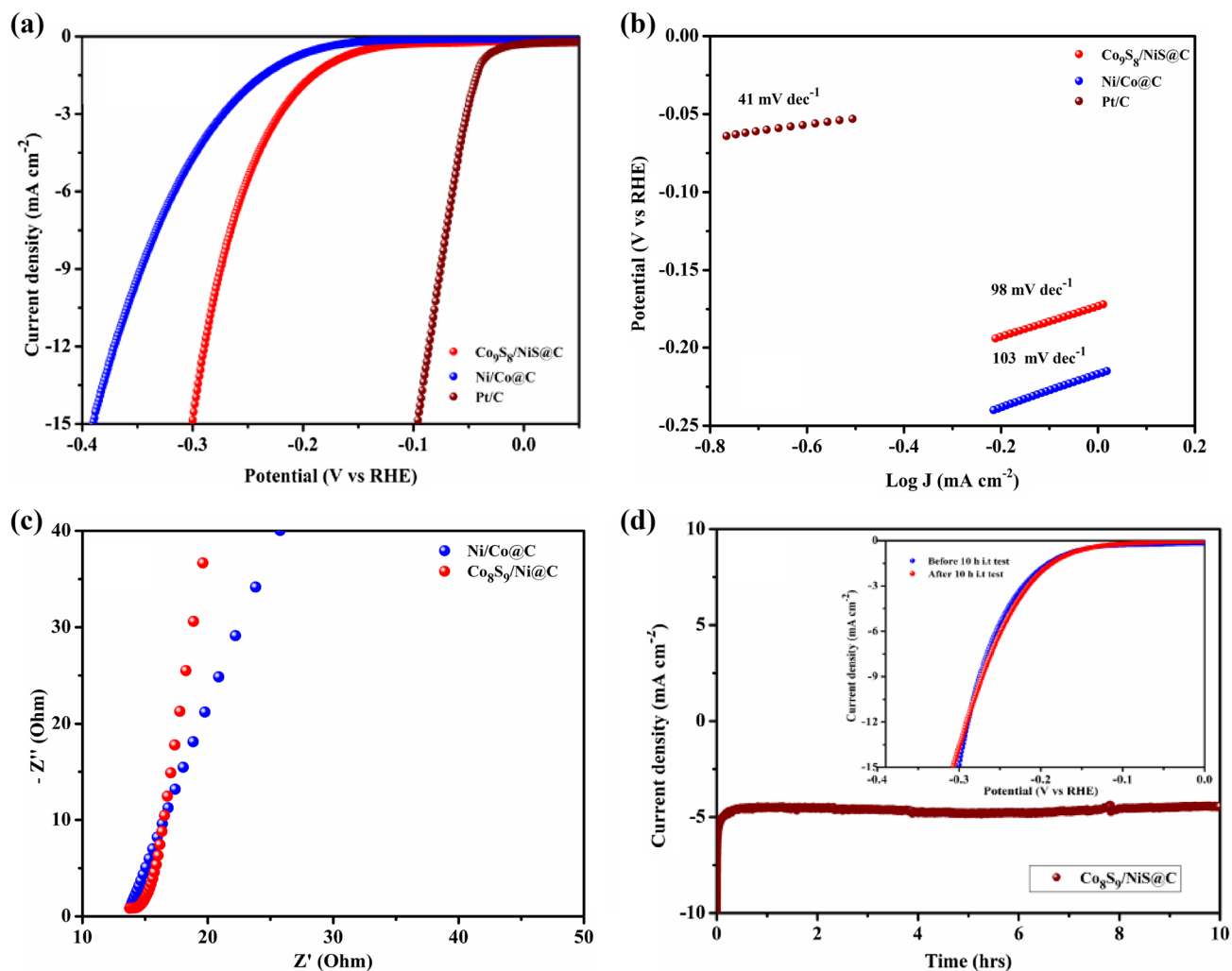


Fig. 5 Electrochemical characterizations: **a** LSV, **b** Tafel plot, **c** EIS measurements and **d** chronoamperometric tests for 10 h for HER of $\text{Co}_9\text{S}_8/\text{NiS}@C$ and $\text{Ni}/\text{Co}@C$, respectively

Pt/C electrocatalyst is an excellent electrocatalyst for HER with lowest overpotential value, while $\text{Co}_9\text{S}_8/\text{NiS}@C$ shows better performance for HER than $\text{Ni}/\text{Co}@C$. The $\text{Co}_9\text{S}_8/\text{NiS}@C$ electrocatalyst shows low overpotential of 0.28 V (vs. RHE) and obtain current density of 10 mA cm^{-2} , and is lower than Pt/C catalyst with overpotential of 0.08 V and higher than $\text{Ni}/\text{Co}@C$ as 0.35 V (vs. RHE), at 10 mA cm^{-2} current density. For better understandings of the kinetic of HER, a linear portion of Tafel plot is used to calculate Tafel slopes from LSV curve following the equation $\eta = b \log j + a$, where j is current density and b is the Tafel slope. Tafel slope value for $\text{Co}_9\text{S}_8/\text{NiS}@C$, $\text{Ni}/\text{Co}@C$ and Pt/C are 98, 103 and 41 mV dec^{-1} , respectively for HER in an alkaline solution (1 M KOH), as shown in Fig. 5b.

The excellent performances of $\text{Co}_9\text{S}_8/\text{NiS}@C$ for HER are attributed to: (1) presence of metal sulfide, the metal ions are the active sites for HER performance, while sulfides are electron donating group and increase the electron cloud

which may enhance the performance of HER, (2) mixed metal sulfide shows different phase and crystal structure which provided more and different spots for HER, (3) the carbon layers not only reduced the corrosion but also facilitated the electron transport for enhanced HER, (4) abundant pores on the surface increase surface area and provide close contact for electrolyte with an electrocatalyst and (5) the nano size of the mix metal sulfide may offer large active sites for HER. Electrochemical impedance spectroscopy (Fig. 5c) of $\text{Co}_9\text{S}_8/\text{NiS}@C$ and $\text{Ni}/\text{Co}@C$ electrocatalysts were investigated at open circuit initial potential in $10\text{--}10^5$ Hz frequency range of and 5 mV AC amplitude of. It is clearly seen that both $\text{Co}_9\text{S}_8/\text{NiS}@C$ and Ni/Co electrocatalysts exhibited a tiny semicircle in high-frequency range implying a low diffusion and R_{ct} between electrolyte and $\text{Co}_9\text{S}_8/\text{NiS}@C$ and Ni/Co electrocatalyst [28, 29]. In low-frequency range, $\text{Co}_9\text{S}_8/\text{NiS}@C$ and Ni/Co electrocatalysts show almost vertical lines which showed good capacitance

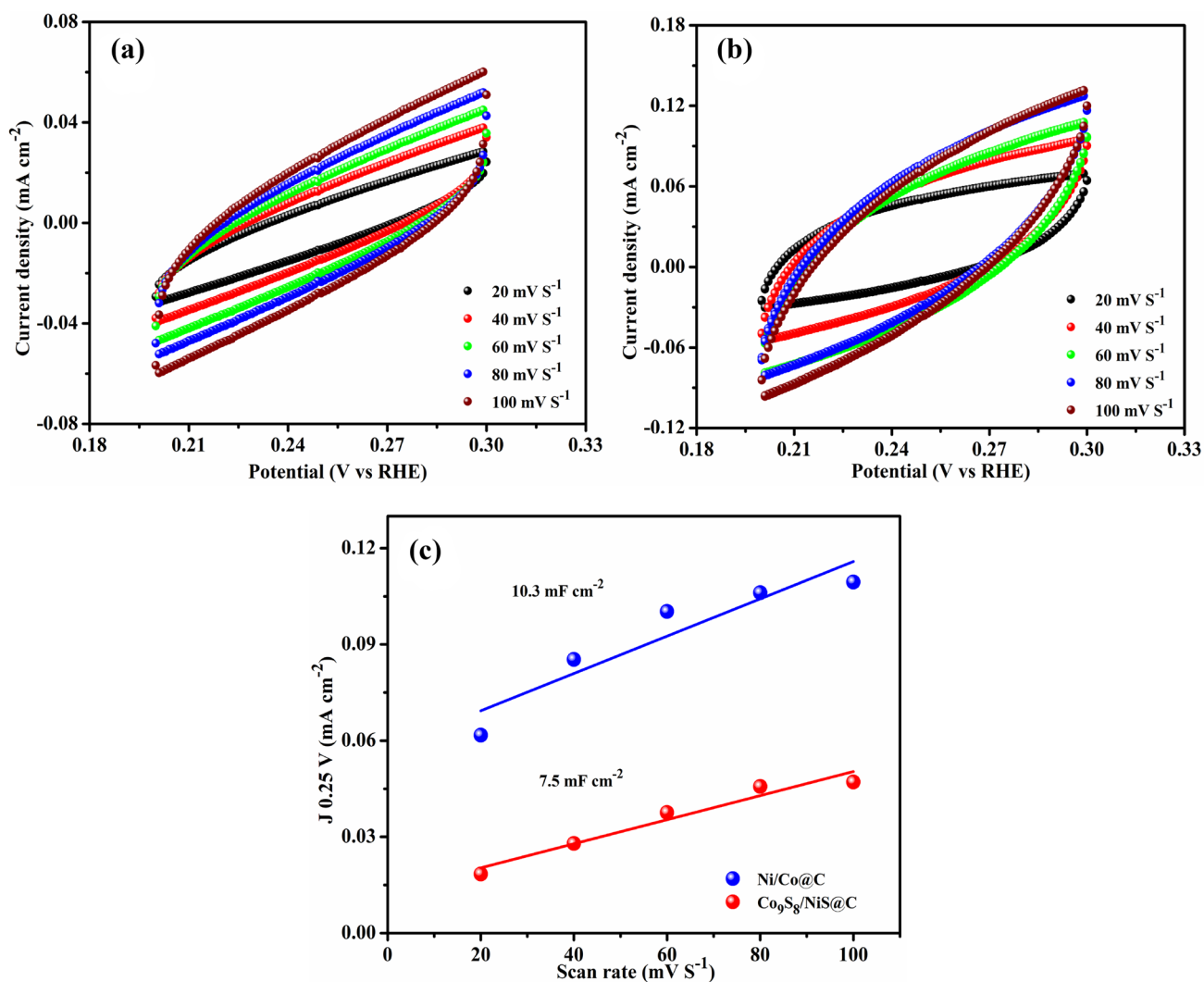


Fig. 6 CV cycles for **a** Co₉S₈/NiS@C, **b** Ni/Co@C and **c** ECSA values

of Co₉S₈/NiS@C and Ni/Co electrocatalysts. The low R_{ct} and good capacitive features of Co₉S₈/NiS@C and Ni/Co might be due to well-scattered nano and micro-sized mixed metal sulfide particles wrapped into carbon layers with abundant surface pores. Mixed metal sulfides facilitates active site for reaction while carbon accelerates transport of electron [28, 30].

Another important factor for evaluation of energy storage performances is the stability of the as-synthesized electrode. For electrocatalyst, the chronoamperometric technique is used to check the stability of 1 M KOH Co₉S₈/NiS@C at 10 mA cm⁻² current density of for 10 h. Figure 5d shows a sharp decline in current density initially due to hydrogen bubble formation on the surface of electrode which inhibited flow of current, while current stabilizes after a short time with the release of hydrogen bubble at a constant rate. The chronoamperometric results show good stability of Co₉S₈/

NiS@C electrocatalyst for 10 h. The stability of Co₉S₈/NiS@C checked with LSV after 10 h showed almost the same overpotential at 10 mA cm⁻² current density, as shown in *inset* Fig. 3d. The electrochemical active surface area of the Co₉S₈/NiS@C and Ni/Co@C are obtained by double layer capacitance (C_{dl}) and half of the obtained C_{dl} value is considered the ECSA of the concern sample [31, 32]. To evaluate C_{dl} value, the Co₉S₈/NiS@C and Ni/Co@C catalysts are CV scanned at 20, 40, 60, 80, and 100 mV s⁻¹ in non-faradic range of 0.2 to 0.3 V (vs. RHE), as shown in Fig. 6a, b. The calculated values of ECSA of Co₉S₈/NiS@C and Ni/Co@C are 1.875 and 2.590 mF cm⁻² (Fig. 6c), respectively. The ECSA results show that Ni/Co@C electrode exhibited high ECSA value than Co₉S₈/NiS@C, which is in accordance with the BET results. The high ECSA value and low HER performance of Ni/Co@C may be due to the presence of carbon that acts as active sites facilitating HER

performance [6]. The excellent HER measurements confirm that mixed metal sulfides with provide more active sites for electro-activity and potential materials for hydrogen evolution reaction systems.

4 Conclusions

One step, simple synthesis and low-temperature pyrolysis method was employed to prepare mixed-metal sulfides $\text{Co}_9\text{S}_8/\text{NiS}@C$ a proficient electrocatalyst for (HER) hydrogen evolution reaction. The obtained mixed metal sulfides are cover with the carbon layer and showed irregular multi-shaped structure. The mixed metal sulfides (Ni–Co–S) nanoparticles wrapped in carbon layers are considered potential electrocatalytic active sites for HER performances showing overpotential of 0.28 V (vs. RHE) to deliver current density of 10 mA cm^{-2} . The $\text{Co}_9\text{S}_8/\text{NiS}@C$ also showed low R_{ct} with good stability for 10 h continuously. The excellent HER activity of $\text{Co}_9\text{S}_8/\text{NiS}@C$ was attributed to the presence of different shape, phase, and crystal structure of mixed metal sulfide assembly. In $\text{Co}_9\text{S}_8/\text{NiS}@C$, the carbon not only protects the metal sulfide corrosion but also facilitate the transport of electron during HER.

Acknowledgements This work was supported by the National Natural Science Foundation of China (51572111, 11774136, 51604049), Natural Science Foundation of Jiangsu Province (Grant No. BK20161347), the Six Talent Peaks Project (TD-XCL-004), the 333 Talents project (BRA2017387), the Innovation/Entrepreneurship Program ([2015]26) and the Qing Lan Project ([2016]15) of Jiangsu Province.

References

1. L. Zhang, W. Liu, Y. Dou, Z. Du, M. Shao, The role of transition metal and nitrogen in metal–N–C composites for hydrogen evolution reaction at universal pHs. *J. Phys. Chem. C* **120**, 29047–29053 (2016)
2. M. Zhuang, X. Ou, Y. Dou, L. Zhang, Q. Zhang, R. Wu et al., Polymer-embedded fabrication of Co_2P nanoparticles encapsulated in N, P-doped graphene for hydrogen generation. *Nano Lett.* **16**, 4691–4698 (2016)
3. X. Li, H. Lei, X. Guo, X. Zhao, S. Ding, X. Gao et al., Graphene-supported pyrene-modified cobalt corrole with a triphenylphosphine axial ligand for enhanced hydrogen evolution in pH 0–14 aqueous solutions. *ChemSuschem* **10**(22), 4632–4641 (2017)
4. D. Huang, J. Lu, S. Li, Y. Luo, C. Zhao, B. Hu et al., Fabrication of cobalt porphyrin. Electrochemically reduced graphene oxide hybrid Films for electrocatalytic hydrogen evolution in aqueous solution. *Langmuir* **30**, 6990–6998 (2014)
5. D. Chanda, J. Hnát, A.S. Dobrota, I.A. Pašti, M. Paidar, K. Bouzek, The effect of surface modification by reduced graphene oxide on the electrocatalytic activity of nickel towards the hydrogen evolution reaction. *Phys. Chem. Chem. Phys.* **17**, 26864–26874 (2015)
6. L. Wang, Y. Li, M. Xia, Z. Li, Z. Chen, Z. Ma et al., Ni nanoparticles supported on graphene layers: an excellent 3D electrode for hydrogen evolution reaction in alkaline solution. *J. Power Sour.* **347**, 220–228 (2017)
7. R. Nivetha, S. Chella, P. Kollu, S.K. Jeong, A. Bhatnagar, N.G. Andrews, Cobalt and nickel ferrites based graphene nanocomposites for electrochemical hydrogen evolution. *J. Magn. Magn. Mater.* **448**, 165–171 (2018)
8. H. Fei, Y. Yang, Z. Peng, G. Ruan, Q. Zhong, L. Li et al., Cobalt nanoparticles embedded in nitrogen-doped carbon for the hydrogen evolution reaction. *ACS Appl. Mater. Interfaces* **7**, 8083–8087 (2015)
9. L. Wang, Y. Li, X. Yin, Y. Wang, A. Song, Z. Ma et al., Coral-like-structured $\text{Ni}/\text{C}_3\text{N}_4$ composite coating: an active electrocatalyst for hydrogen evolution reaction in alkaline solution. *ACS Sustain. Chem. Eng.* **5**, 7993–8003 (2017)
10. Z. Chen, L. Wang, Z. Ma, J. Song, G. Shao, Ni-reduced graphene oxide composite cathodes with new hierarchical morphologies for electrocatalytic hydrogen generation in alkaline media. *RSC Adv.* **7**, 704–711 (2017)
11. S. Peng, L. Li, X. Han, W. Sun, M. Srinivasan, S.G. Mhaisalkar et al., Cobalt sulfide nanosheet/graphene/carbon nanotube nanocomposites as flexible electrodes for hydrogen evolution. *Angew. Chem. Int. Ed.* **53**, 12594–12599 (2014)
12. L. Wang, Y. Li, X. Yin, Y. Wang, L. Lu, A. Song et al., Comparison of three nickel-based carbon composite catalysts for hydrogen evolution reaction in alkaline solution. *Int. J. Hydrog. Energy* **42**, 22655–22662 (2017)
13. Cai Zx, Xh Song, Wang Yr, X. Chen, Electrodeposition-assisted synthesis of Ni_2P nanosheets on 3D graphene/Ni foam electrode and its performance for electrocatalytic hydrogen production. *ChemElectroChem* **2**, 1665–1671 (2015)
14. R.K. Shervedani, M. Torabi, F. Yaghoobi, Binder-free prickly nickel nanostructured/reduced graphene oxide composite: a highly efficient electrocatalyst for hydrogen evolution reaction in alkaline solutions. *Electrochim. Acta* **244**, 230–238 (2017)
15. J. Yang, C. Cai, Y. Li, L. Gao, H. Guo, B. Wang et al., In-situ cobalt and nitrogen doped mesoporous graphitic carbon electrocatalyst via directly pyrolyzing hyperbranched cobalt phthalocyanine for hydrogen evolution reaction. *Electrochim. Acta* **262**, 48–56 (2018)
16. H.J. Qiu, Y. Ito, W. Cong, Y. Tan, P. Liu, A. Hirata et al., Nanoporous graphene with single-atom nickel dopants: an efficient and stable catalyst for electrochemical hydrogen production. *Angew. Chem. Int. Ed.* **54**, 14031–14035 (2015)
17. B. Rezaei, A.R.T. Jahromi, A.A. Ensafi, Ni–Co–Se nanoparticles modified reduced graphene oxide nanoflakes, an advance electrocatalyst for highly efficient hydrogen evolution reaction. *Electrochim. Acta* **213**, 23–31 (2016)
18. W. Yuan, X. Wang, X. Zhong, C.M. Li, CoP nanoparticles in situ grown in three-dimensional hierarchical nanoporous carbons as superior electrocatalysts for hydrogen evolution. *ACS Appl. Mater. Interfaces* **8**, 20720–20729 (2016)
19. S. Badrayyana, D.K. Bhat, S. Shenoy, Y. Ullal, Novel Fe–Ni-graphene composite electrode for hydrogen production. *Int. J. Hydrog. Energy* **40**, 10453–10462 (2015)
20. X. Long, G. Li, Z. Wang, H. Zhu, T. Zhang, S. Xiao et al., Metallic iron–nickel sulfide ultrathin nanosheets as a highly active electrocatalyst for hydrogen evolution reaction in acidic media. *J. Am. Chem. Soc.* **137**, 11900–11903 (2015)
21. C.-K. Cheng, T.-K. Yeh, M.-C. Tsai, H.-Y. Chou, H.-C. Wu, C.-K. Hsieh, The hybrid nanostructure of vertically aligned cobalt sulfide nanoneedles on three-dimensional graphene decorated nickel foam for high performance methanol oxidation. *Surf. Coat. Technol.* **320**, 536–541 (2017)
22. Y.-R. Liu, W.-H. Hu, X. Li, B. Dong, X. Shang, G.-Q. Han et al., Facile one-pot synthesis of CoS_2 – MoS_2 /CNTs as efficient

- electrocatalyst for hydrogen evolution reaction. *Appl. Surf. Sci.* **384**, 51–57 (2016)
23. Z. Ma, Q. Zhao, J. Li, B. Tang, Z. Zhang, X. Wang, Three-dimensional well-mixed/highly-densed NiS–CoS nanorod arrays: an efficient and stable bifunctional electrocatalyst for hydrogen and oxygen evolution reactions. *Electrochim. Acta* **260**, 82–91 (2018)
24. C. Zequine, S. Bhoyate, K. Siam, P.K. Kahol, N. Kostoglou, C. Mitterer et al., Needle grass array of nanostructured nickel cobalt sulfide electrode for clean energy generation. *Surf. Coat. Technol.* **354**, 306–312 (2018)
25. S. Shit, S. Chhetri, W. Jang, N.C. Murmu, H. Koo, Cobalt sulfide/nickel sulfide heterostructure directly grown on nickel foam: an efficient and durable electrocatalyst for overall water splitting application. *ACS Appl. Mater. Interfaces* **10**, 27712–27722 (2018)
26. C. Yu, Y. Wang, J. Zhang, W. Yang, X. Shu, Y. Qin et al., One-step electrodeposition of $\text{Co}_{0.12}\text{Ni}_{1.88}\text{S}_2@\text{Co}_8\text{S}_9$ nanoparticles on highly conductive TiO_2 nanotube arrays for battery-type electrodes with enhanced energy storage performance. *J. Power Sour.* **364**, 400–409 (2017)
27. X. Huang, J. Wang, H. Bao, X. Zhang, Y. Huang, 3D nitrogen, sulfur-codoped carbon nanomaterial-supported cobalt oxides with polyhedron-like particles grafted onto graphene layers as highly active bicalysts for oxygen-evolving reactions. *ACS Appl. Mater. Interfaces* **10**, 7180–7190 (2018)
28. Y. Li, Z. Li, P.K. Shen, Simultaneous formation of ultrahigh surface area and three-dimensional hierarchical porous graphene-like networks for fast and highly stable supercapacitors. *Adv. Mater.* **25**, 2474–2480 (2013)
29. M. Yu, J. Chen, J. Liu, S. Li, Y. Ma, J. Zhang et al., Mesoporous NiCo_2O_4 nanoneedles grown on 3D graphene-nickel foam for supercapacitor and methanol electro-oxidation. *Electrochim. Acta* **151**, 99–108 (2015)
30. S. Hussain, T. Liu, M.S. Javed, N. Aslam, N. Shaheen, S. Zhao et al., Amaryllis-like NiCo_2S_4 nanoflowers for high-performance flexible carbon-fiber-based solid-state supercapacitor. *Ceram. Int.* **42**, 11851–11857 (2016)
31. X. Wang, Y. Chen, B. Zheng, F. Qi, J. He, Q. Li, Graphene-like WSe_2 nanosheets for efficient and stable hydrogen evolution. *J. Alloys Compd.* **691**, 698–704 (2017)
32. S. Hussain, M.S. Javed, N. Ullah, A. Shaheen, N. Aslam, I. Ashraf, Y. Abbas, M.S. Wang, G.W. Liu, G.J. Qiao, Unique hierarchical mesoporous LaCrO_3 perovskite oxides for highly efficient electrochemical energy storage applications. *Ceram. Int.* **45**, 15164–15170 (2019)

Publisher's Note Springer Nature remains neutral with regard to jurisdictional claims in published maps and institutional affiliations.